Copolymerization of β-butyrolactones into functionalized polyhydroxyalkanoates using aluminum catalysts: influence of the initiator in the ring-opening polymerization mechanism

Miguel Palenzuela, Esther Mula, Carlos Blanco, Valentina Sessini, Rama M. Shakaroun, Hui Li, Sophie M. Guillaume, Marta E. G. Mosquera

Macromolecular Rapid Communications
www.mrc-journal.de

Copolymerization of β-Butyrolactones into Functionalized Polyhydroxyalkanoates Using Aluminum Catalysts: Influence of the Initiator in the Ring-Opening Polymerization Mechanism

*Miguel Palenzuela, Esther Mula, Carlos Blanco, Valentina Sessini, Rama M. Shakaroun, Hui Li, Sophie M. Guillaume, and Marta E. G. Mosquera**

Within bioplastics, natural poly(3-hydroxybutyrate) (PHB) stands out as fully biocompatible and biodegradable, even in marine environments; however, its high isotacticity and crystallinity limits its mechanical properties and hence its applications. PHB can also be synthesized with different tacticities via a catalytic ring-opening polymerization (ROP) of *rac*-β-butyrolactone (BBL), paving the way to PHB with better thermomechanical and processability properties. In this work, the catalyst family is extended based on aluminum phenoxy-imine methyl catalyst [AlMeL_2], that reveals efficient in the ROP of BBL, to the halogeno analogous complex [AlClL_2]. As well, the impact on the ROP mechanism of different initiators is further explored with a particular focus in dimethylaminopyridine (DMAP), a hardly studied initiator for the ROP of BBL. A thorough mechanistic study is performed that evidences the presence of two concomitant DMAP-mediated mechanisms, that lead to either a DMAP or a crotonate end-capping group. Besides, in order to increase the possibilities of PHB post-polymerization functionalization, the introduction of a side-chain functionality is explored, establishing the copolymerization of BBL with β-allyloxymethylene propiolactone (BPL^{OAll}), resulting in well-defined P(BBL-*co*-BPL^{OAll}) copolymers.

1. Introduction

Plastics are versatile and useful materials that are present in many aspects of our everyday life. However, some of their main characteristics, their durability and high performance, have led to a lack of recyclability and/or biodegradability, ultimately resulting in a major environmental issue. Biodegradation under controlled conditions such as composting is one feasible alternative to the constant accumulation of plastics waste that spreads throughout the planet. In particular, synthetic materials that can also degrade in natural environments, such as marine ones, are of great interest.[1–3]

A well-known type of naturally produced and biodegradable polymers are polyhydroxyalkanoates (PHAs).[4,5] The most ubiquitous one, poly(3-hydroxybutyrate) (PHB), is a material produced from biomass by some bacteria, and it is accumulated in granules inside cells then serving as energy feedstock.[6,7] In addition, while being biodegradable, even in aqueous environments, PHB is fully biocompatible.[8–10] However, the naturally produced PHB is highly isotactic, hard and brittle with a high crystallinity and low elongation at break.[9] These thermomechanical properties thus limit its industrial applications.[4,11–14]

PHB can also be synthetically produced via catalytic ring-opening polymerization (ROP) of four-membered ring β-lactones.[15,16] This synthetic pathway can return PHB with different tacticities, paving the way to the generation of PHB with improved thermomechanical and processability properties. In particular, it is possible to produce PHB from β-butyrolactone (BBL), although it is a challenging monomer to polymerize. As such, due to its relative strained cycle as compared to larger cyclic esters that more easily undergo ROP, only a few examples of efficient catalysts for the ROP of BBL have been reported.[17–20] These polymerizations have been mainly mediated by anionic initiators, or by discrete metal complexes, the latter ones affording a better control of the polymer features, especially in terms of dispersity and stereoregularity of the polymers microstructure. In particular, organometallic compounds

M. Palenzuela, E. Mula, C. Blanco, V. Sessini, M. E. G. Mosquera
Departamento de Química Orgánica y Química Inorgánica, Instituto de Investigación en Química "Andrés M. del Río" (IQAR), Universidad de Alcalá
Campus Universitario
Alcalá de Henares, Madrid 28871, Spain
E-mail: martaeg.mosquera@uah.es
R. M. Shakaroun, H. Li, S. M. Guillaume
Univ. Rennes, CNRS
Institut des Sciences Chimiques de Rennes
UMR 6226, Rennes F-35042, France

The ORCID identification number(s) for the author(s) of this article can be found under https://doi.org/10.1002/marc.202400091

DOI: 10.1002/marc.202400091

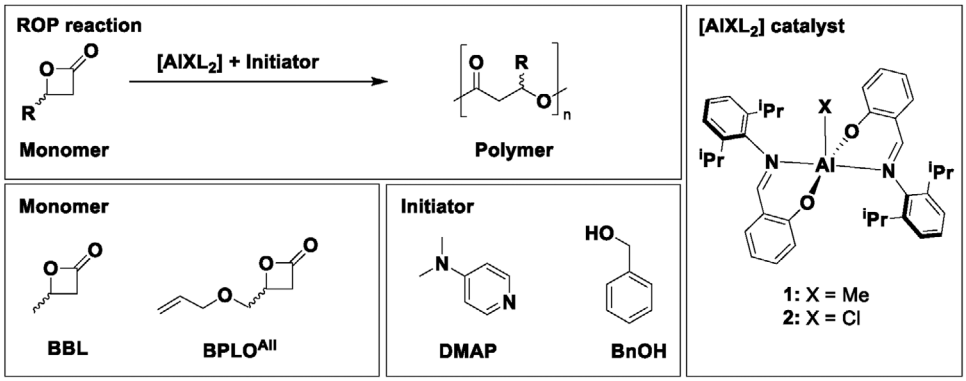

Figure 1. Catalysts, initiators, and monomers used in the present study.

of different metals such as yttrium,[21–25] lanthanum,[26] titanium, zirconium and hafnium,[27,28] chromium,[29,30] tin,[31–36] magnesium,[37] aluminium,[38–43] zinc,[37,44] and indium,[45] have been described as active catalysts for the ROP of BBL.

In order to enhance the properties of PHB, an effective strategy relies on the introduction of side chain functionalities. Implementation of a substituent on the repeating units throughout the polymer backbone can affect the properties, especially the solubility, crystallinity, thermal and mechanical features as well as the degradation profile. Besides, such pending functional groups may enable post-polymerization modifications. Homopolymers and copolymers with a variable degree of functionalization can thus be prepared by ROP and ring-opening copolymerization (ROCOP) of functionalized β-lactones, respectively. The effective synthesis of functionalized β-lactones, especially through carbonylation of the corresponding epoxide, and their subsequent ROP have thus enabled the preparation of various PHAs.[26,46–50]

We have previously established a series of main group metals phenoxyimine compounds as effective catalysts in the ROP of lactones.[38,51–54] In particular, we have reported that the aluminium phenoxyimine methyl derivative [$AlMeL_2$] (**1**) (**Figure 1**) is an active catalyst for the ROP of *rac*-BBL as well as for its ROCOP with L-lactide (LLA) or ϵ-caprolactone (CL), in the presence of BnOH as initiator.[38,53] Quantitative monomer(s) conversions in toluene solution at 100 °C were achieved at a catalyst-to-monomer loading ratio of 1:100 within 5 h (turn over frequency (TOF) = 18.0 h^{-1}),[38] thereby establishing one of the most active aluminium complexes for the ROP of BBL (Table S1, Supporting Information). Compound **1** featuring two phenoxo imino ancillary ligands presents a pentacoordinated aluminum within a geometry around the metal that is more flexible and labile in comparison to the one with only one ligand – as within the analogous salen derivatives, thereby promoting efficiently the ROP of cyclic esters.[55,56]

The remarkable activity of **1** in the ROP and ROCOP of BBL prompted us to investigate its activity toward the functionalized β-lactone, β-allyloxymethylene propiolactone (BPL^{OAll}), both in homopolymerization and copolymerization with BBL, to access to functionalized polyesters. Also, we have comparatively assessed the activity of the chloro analogue of **1**, namely [$AlClL_2$] (**2**). Furthermore, we have broadened our studies to an initiator of different nature (non protonic) such as dimethylaminopyridine (DMAP) to analyze its influence on the polymerization mechanism. Interestingly, DMAP has hardly been studied as initiator for the ROP of BBL; in fact, it has only been reported for Zn catalysts exhibiting high initiation efficiency for lactide ROP.[57,58]

2. Results and Discussion

2.1. Synthesis of the Aluminum Phenoxyimine Complexes [$AlXL_2$] (X = Me (1), Cl (2))

The methyl aluminum complex **1**, [$AlMeL_2$], was synthesized following our previously published methodology, via the reaction of the phenoxyimine ligand precursor with $AlMe_3$, while its chloro parent complex **2**, [$AlClL_2$], was prepared in a similar way using $AlMe_2Cl$ as the aluminum precursor (**Scheme 1**).

The herein newly prepared compound **2** was characterized by analytical and spectroscopic methods (see Figures S1–S5, Supporting Information). ^1H NMR analysis clearly showed the disappearance of the ligand-OH signal at δ 12.67 ppm and of the upfield Al-methyl signal, supporting the formation of the chloride derivative. Also, the resonances corresponding to the ligand are shifted from those of the precursor ones, particularly the hydrogens from the HC=N and the $HC(CH_3)_2$ groups which moved downfield, further suggesting the bonding to the aluminum upon formation of species **2**. Noteworthy, two different NMR signals were observed for the isopropyl groups, resulting from the presence of an intramolecular hydrogen bond between the hydrogen atom of the methine moieties from only one isopropyl substituent and the chloride, that may restrict the free rotation around the N—Ar bond. This feature results in non-equivalent isopropyl groups.

This observation was confirmed from the solid-state structure of crystals of **2**, as determined by X-ray diffraction analysis (**Figure 2**). Three identical molecules are present in the unit cell, one of them showing some positional disorder. In this molecule, the aluminum atom is pentacoordinated, with a distorted square-based pyramid geometry. The ligands donor atoms, oxygen and nitrogen, are nearly coplanar and form the base of the pyramid with the chlorine atom at the apex. The Al—Cl bond distance in the non-disordered molecule (2.1640(9) Å), is within the range of values reported for half-salen chloro-derivatives (2.104–2.219 Å).[59–62] Al—O and Al—N bond lengths are also in the classical range while, as observed for compound **1**, the Al—O bonds

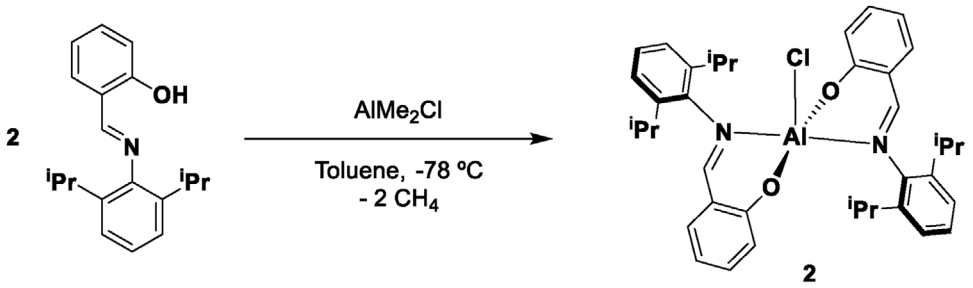

Scheme 1. Synthesis of the [$AlClL_2$] complex **2**.

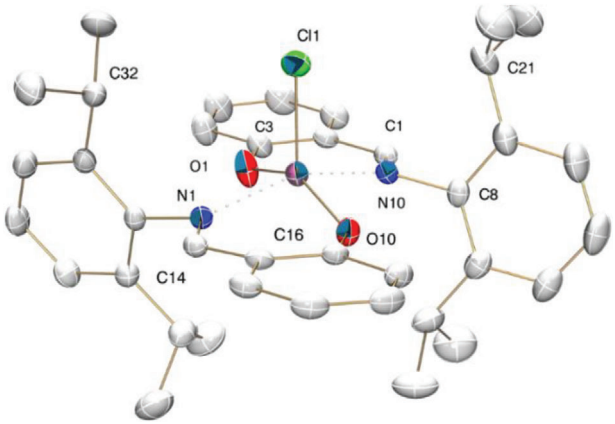

Figure 2. ORTEP plot of **2** showing thermal ellipsoid plots (30% probability). Hydrogen atoms have been omitted for clarity. Selected bond lengths (Å) and angles (°) for the disordered molecule: Al(1)-O(1), 1.7599(17); Al(1)-O(10), 1.7636(16); Al(1)-Cl(1), 2.1640 (9); Al(1)-N(1), 2.0451(18); Al(1)-N(10), 2.058(18); O(1)-C(3), 1.314(3); O(10)-C(16),1.324(2); N(1)-C(14), 1.289(3); N(10)-C(1), 1.292(3); O(1)-Al(1)-N(1), 84.07(7); O(10)-Al(1)-N(1), 88.06(7); O(10)-Al(1)-N(10), 85.68(7); O(1)-Al(1)-N(10), 88.42(8); O(1)-Al(1)-Cl(1), 106.92(8); O(10)-Al(1)-Cl(1), 106.71(6); N(1)-Al(1)-Cl(1), 100.82(6); N(10)-Al(1)-Cl(1), 103.03(6).

(1.7599(17) and 1.7636(16) Å) fall within the shortest ones (1.75 to 1.85 Å), and Al—N ones, although shorter than in **1** (**1**: 2.107(6) to 2.123(6) Å; **2**: 2.0457(18) and 2.052(18) Å)), are still among the longest ones reported (1.95 to 2.15 Å range).[63] As pointed out in the molecular structure of **1**, this structural peculiarity could result in the lability of the Al—N bonds.[38]

In the X-ray crystal structure of **2**, two out of four isopropyl groups are oriented toward the chloride ligand with the geometry suitable for a H-bond interaction, in agreement with the behavior observed from NMR analysis.

2.2. Polymerization of BBL Mediated by [$AlXL_2$] Catalysts (X = Me (1), Cl (2)) and DMAP

We then investigated the catalytic ROP of BBL mediated by catalysts **1** and **2** in the presence of DMAP as initiator. Even though DMAP is a well-known organocatalyst for ROP processes, it has surprisingly hardly been reported as an initiator for the ROP of BBL catalyzed by metal complexes, only with Zn compounds.[57,58]

The polymerization of *rac*-BBL mediated by **1** was performed in bulk with a 100:1:1 monomer/catalyst/initiator ratio at a temperature ranging from 100 to 130 °C (only poor conversion < 10% was observed below 100 °C). At 100 °C, quantitative monomer conversion was achieved in 90 min (**Table 1**, entry 3) to give PHB with a moderate dispersity ($M_{n,SEC}$ (kDa) = 3.3; $Đ$ = 1.24; Table 1, entry 3). The ROP at a higher monomer loading of 200 equivalents (Table 1, entry 4), resulted in lower BBL conversions at 120 min; this effect has been previously observed and could be attributed to mass transfer problems in the reaction media.[19,38] Raising the reaction temperature to 130 °C enabled to reach full conversion more rapidly, as anticipated, but shorter chains were then formed ($M_{n,SEC}$ (kDa) = 2.1, Table 1, entry 5), probably due to transesterification reactions that are typically favored at higher temperature, and/or to chain transfer reactions faster than the propagation.

For compound **1**, in comparison to the results obtained using BnOH as initiator under the same operating conditions,[38] DMAP clearly accelerated the ROP, enabling the polymerization to proceed in 90 instead of 300 min (Table 1, entry 6). However, the results from DMAP indicated a poorer control over the process, as suggested by the experimental molar mass values which remained twice as low as the expected ones, and the dispersity which was significantly higher than for the **1**/BnOH system ($M_{n,SEC}$ (kDa) = 7.4; $Đ$: 1.03; Table 1, entry 6).[38]

For comparison, we also performed the ROP of BBL organocatalyzed by DMAP. As shown in entries 1–2, the reaction was slower than when using compound **1** as catalyst: as such, the quantitative conversion was achieved at 130 °C in 2 h. Besides, the polymer formed was significantly shorter ($M_{n,SEC}$ (kDa) = 1.5; Table 1, entry 2), thereby hinting that propagation process is competing with the termination reaction. The increase of the rate of the reaction in the presence of the metal complex has been previously observed for other nucleophilic organic bases acting as organocatalysts, and has been attributed to the coordination of the metal center to the lactone which increases the reactivity of the carbonyl group and facilitate the ROP reaction.[59]

The ROP of BBL mediated by catalyst **2** in the presence of BnOH revealed more sluggish, requiring a longer reaction time at 100 °C to reach high monomer consumption and leading to poor conversion at a higher temperature (Table 1, entries 6, 10). Replacing BnOH by DMAP enabled to reach higher conversions (entries 7–9). At 100°C, more than 60% of BBL was consumed within 2 h; this remained lower than observed with **1** (> 99%), and the polymers recovered were shorter, indicating a poorer con-

Table 1. ROP of BBL catalysed by **1** and **2** in bulk.

Entry	[Al]	[I]	$[Al]_0$:$[I]_0$:$[BBL]_0$	Temp. [°C]	Reaction time [min]	BBL Conv.[a] [%]	$M_{n,theo}$[b] [kDa]	$M_{n,SEC}$[c] [kDa]	$Đ$[c]
1	–	DMAP	0:1:100	100	120	88	7.6	1.2	1.16
2	–	DMAP	0:1:100	130	120	> 99	8.7	1.5	1.47
3	1	DMAP	1:1:100	100	90	98	8.6	3.3	1.24
4	1	DMAP	1:1:200	100	120	78	13.6	4.3	1.21
5	1	DMAP	1:1:100	130	60	> 99	8.6	2.1	1.17
6[38]	1	BnOH	1:1:100	100	300	90	7.8	7.4	1.03
7	2	DMAP	1:1:100	100	120	67	5.9	1.7	1.21
8	2	DMAP	1:1:200	100	120	62	10.8	2.1	1.26
9	2	DMAP	1:1:100	130	120	> 99	8.7	9.31.5	1.11.2
10	2	BnOH	1: 1:100	130	120	14	1.3	–	–

[a] Monomer conversion as determined by ^{1}H NMR spectroscopy; [b] Theoretical molar mass in the presence of initiator: $M_{n,theo}$ = M(I) + M(BBL) %Conv $[BBL]_0/[I]_0$; or theoretical molar mass in the absence of initiator: $M_{n,theo}$ = M(BBL) %Conv $[BBL]_0/[Al]_0$; [c] Molar mass and dispersity determined by SEC in tetrahydrofuran (THF) using polystyrene standard.

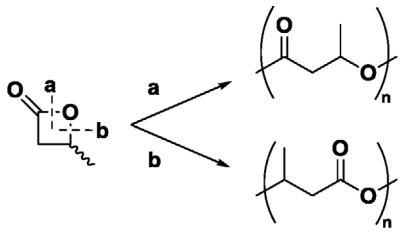

Scheme 2. Two possible pathways for the ROP of BBL upon a) O-acyl bond cleavage, and b) O-alkyl bond cleavage.

trol. With compound **2**, complete conversion was attained within 2 h at 130 °C, yet giving polymers with a bimodal distribution, possibly arising from two concomitant mechanisms contributing to the formation of PHB (see below).

Deeper insight into the ROP mechanism monitored by NMR spectroscopy and mass spectrometry enabled to assess the impact of DMAP as initiator. We have previously established that the mechanism for the **1**/BnOH catalyst system is a typical coordination-insertion (CI) mechanism, where the BBL monomer inserts into the Al—OBn bond in the initiation step.[38] As such, we could isolate the resulting benzyloxy complex, where the methyl group has been substituted by BnO, which subsequently successfully enabled the ROP of BBL returning *α*-hydroxy,*ω*-benzyloxy end-capped PHB.[38] For the Al—Cl derivative, no reaction with the BnOH is observed, which indicates that the formation of the benzyloxy complex is a key step for the catalytic process to take place.

It should be noted that the ROP of BBL can take place by two different pathways: via O-acyl bond cleavage leading to alkoxide terminated chains (**Scheme 2**a), or via O-alkyl bond cleavage (Scheme 2b) giving a carboxylate end-group.

The O-acyl cleavage typically takes place when using organometallic catalysts, according to two possible pathways: coordination-insertion (CIM) or activated monomer (AMM) mechanism (**Scheme 3**).[21–23,30,36–38,40,42,53,64–67] In our case, using DMAP as initiator, both mechanisms would give a polymer featuring a DMAP and a hydroxyl end-groups.[59] As such, for the CIM, the first step implies the coordination of the initiator (DMAP) to the aluminum, followed by the approach of a monomer to the metal, enhancing its electrophilicity and promoting its insertion in the Al-DMAP bond. Afterward, the polymerization reaction proceeds by the consecutive insertion of the monomer into the growing chain-aluminum bond via an O-acyl cleavage (Scheme 3a). In contrast, the AMM proceeds through the nucleophilic attack of the initiator, DMAP, on the carbonyl group of the monomer BBL, which is activated via its interaction with the aluminum centre.[59] The growth of the polymer chain occurs through the nucleophilic attack of the anionic growing chain on successive activated monomer molecules prompting the ring opening (Scheme 3).

The less common O-alkyl cleavage has been typically observed when using potassium anionic species or strong bases as initiators within an anionic ROP mechanism (AROP).[68–73] In the AROP mechanism, the real ROP initiator species is the crotonate, which is the anionic and unsaturated derivative of BBL (**Scheme 4**).[69–74] Formation of crotonate can be readily achieved as DMAP can abstract a proton from BBL (Scheme 4a).[72,74] Besides, in our catalyst system, this deprotonation will be favored by the interaction of the monomer with the aluminum since it enhances the acidity of the carbonyl group.[59] Once the crotonate is formed, it will initiate the propagation of the chain via the O-alkyl cleavage following an AROP mechanism.

To get further insight into the ROP mechanism of BBL mediated by **1**/DMAP, the PHB samples were characterized by NMR spectroscopy and mass spectrometry. A typical ^{1}H NMR spectra of PHB is illustrated in **Figure 3**. The characteristic signals corresponding to the methyl, methylene, and methine of the repeating unit (δ 1.25, 2.40–2.61, and 5.22 ppm, respectively) are clearly observed, along with signals corresponding to both crotonate and DMAP moieties. These observations suggest the presence of two distinct polymeric chains arising from the two concomitant mechanisms involving O-alkyl and O-acyl cleavage of the monomer (Schemes 3 and 4). ^{13}C{^{1}H}, HSQC and HMBC NMR analyzes of the polymer sample (see Figures S8–S12, Supporting Information) confirmed the presence of both a crotonate and a DMAP chain-end groups, in agreement with the presence of two different polymer chains. Besides, DOSY analyzes further

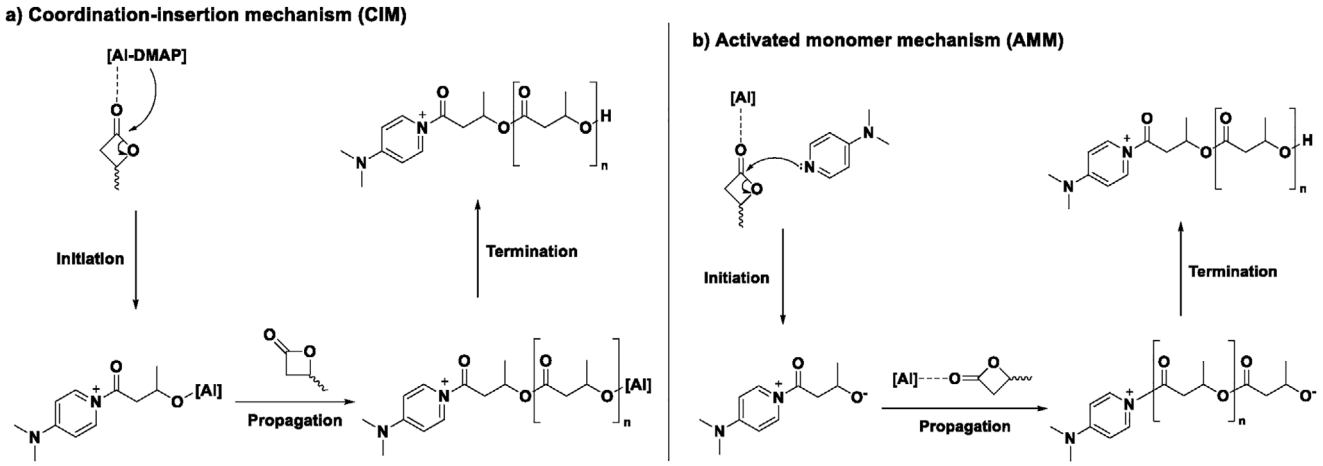

Scheme 3. ROP of BBL with **1**/DMAP catalytic system via O-acyl cleavage: a) Coordination-insertion mechanism (CIM), and b) Activated monomer mechanism (AMM).

confirmed that both these terminal groups were bond to the polymer chains (see Figure S13, Supporting Information). Estimation of the relative amount of each end-group by ^{1}H NMR spectra, gave a crotonate/DMAP ratio of 9:1 and 13:1 for the polymers obtained using **1**/DMAP, and **2**/DMAP, respectively, indicating that the O-alkyl cleavage via an AROP mechanism prevailed in both cases (see Figures S8 and S14, Supporting Information). The formation of non-covalent interactions between the carboxylate group of the crotonate and the metal center may contribute to stabilize intermediate species, thereby favoring this mechanism. When using only DMAP as organocatalyst, the ^{1}H NMR spectrum of the purified polymer showed the presence of crotonate and DMAP terminated chains in a 1:1 ratio (see Figure S20, Supporting Information). Hence, in this case, both cleavages are equally occurring, without any preference for the O-alkyl rupture as when the aluminum catalyst was present.

Polymer chains end-capped with DMAP and resulting from the O-acyl cleavage, may arise from either a CIM or AMM (see Scheme 3a,b). In order to clarify the role of the initiator in the ROP process, we studied the stoichiometric reactions of the aluminum compounds and DMAP. ^{1}H NMR signals characteristic of complexes **1**, **2** and of DMAP remained unshifted (see Figures S6 and S7, Supporting Information) suggesting that DMAP does not coordinate to the aluminum center in **1** nor in **2**. Hence, the

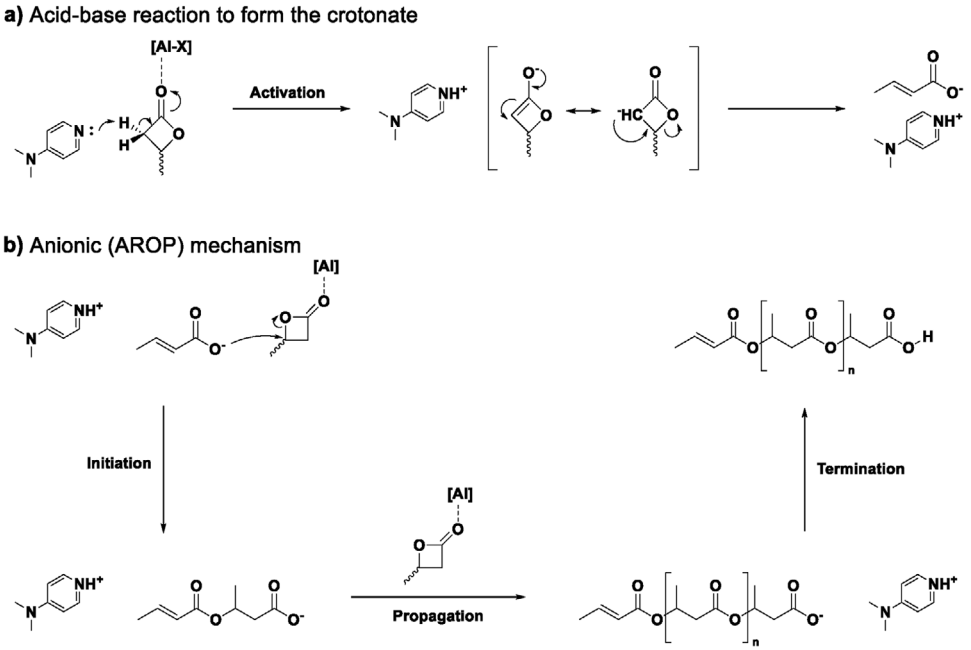

Scheme 4. a) Acid-base reaction of BBL and DMAP in the presence of the aluminum complex to give the corresponding pyridinium crotonate species ([DMAP-H]$^+$ [crotonate]$^-$). b) Anionic (AROP) mechanism for the ROP of BBL with the [Al]/DMAP catalytic systems via the O-alkyl cleavage through the formation of the crotonate BBL anionic derivative, resulting in α-crotonyl,ω-carboxyl end-capped PHB.

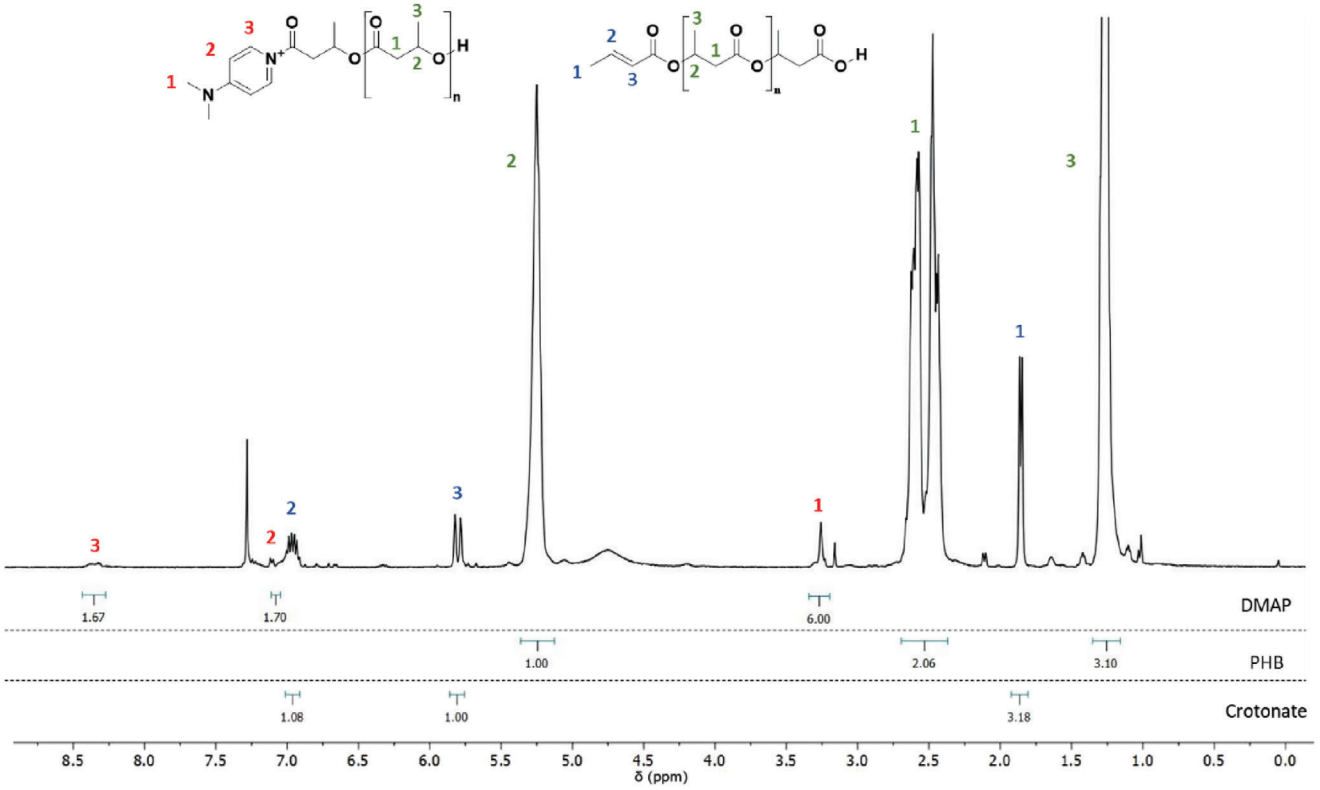

Figure 3. ^{1}H NMR spectrum (400 MHz, $CDCl_3$, 293 K) of a purified PHB sample prepared by ROP of BBL mediated by **1**/DMAP at 100 °C in bulk, showing both crotonate and DMAP chain end-groups (Table 1, entry 3).

O-acyl cleavage route does not proceed through a CIM, as reported for **1**/BnOH,[38] but since DMAP was found as a polymer end-capping group, as confirmed by the DOSY experiments, the reaction may rather proceed through an AMM, where DMAP behaves as a nucleophile, attacking the carbonyl group along with O-acyl bond cleavage.

MALDI-TOF mass spectrometry analyzes of a PHB sample prepared by ROP of BBL catalyzed by **1**/DMAP (Table 1, entry 3, **Figure 4**) displayed a major population attributed to $[DMAP(C_4H_6O_2)_nH]^+$, corresponding to a PHB end-capped with dimethylamino pyridinium and hydroxyl groups (Figures S8–S10, Supporting Information). Additionally, the minor population identified as $[(C_4H_6O_2)_nNa]^+$, corresponds to *α*-crotonate,*ω*-carboxylic PHB arising from an AROP mechanism (Scheme 3).[69–73] In all cases, the population corresponding to DMAP chain-ends is significantly more intense, an effect which could be attributed to the fact that the uncharged chains can be obscured by the charged polymer chains with DMAP end-caps, as previously reported.[75] The concomitance of two mechanisms thus rationalizes the lower control of the molar mass values, in comparison to the previously reported **1**/BnOH catalyst system.[38]

The stereochemistry of the polymers was next investigated by ^{13}C NMR spectroscopy. The calculation using the integration area of the corresponding signals of the polymers enabled to determine the stereoregularity of the samples (**Figure 5**; Figures S40–S42, Supporting Information). For the methylene region: $P_r = 2\,(rr)/[2\,(rr) + rm + mr]$; $rm = mr = P_r\,(1 - P_r)$; $mm = (1 - P_r)$[2] $rr = Pr^2$,[76] and for the carbonyl region: $P_r = (r)/[(r) + (m)]$.[64,67] In our case, for the polymer obtained with **1**/DMAP, the tacticity obtained from the probability of a racemic diad or triad gives the same value of $P_r = 0.51$. However, the P_r values of the other polymers obtained with **2**/DMAP, and with only DMAP (no catalyst), showed slight differences in both regions (**2**/DMAP $P_r^{CO} = 0.56$ and $P_r^{CH2} = 0.46$; versus DMAP $P_r^{CO} = 0.44$ and $P_r^{CH2} = 0.51$). Such an observation has been previously described and could be attributed to the overlapping of NMR signals that can limit – to some extent – the reliability of the integration values.[77] Even so, these values revealed the atactic character ($P_r \approx 0.5$) of the PHBs obtained with the different catalytic systems.

Additionally, we can understand the chain-end control through the Bernoulli triad model test reported (see Tables S2–S7, Supporting Information) where $B = 4(mm)(rr)/[(rm) + (mr)^2]$.[78] The results obtained ($B_{1/DMAP} = 1.03$, $B_{2/DMAP} = 0.81$ and $B_{DMAP} = 0.68$) showed that a very high control is reached in the reaction catalysed by **1**/DMAP, since the value obtained is very close to 1, which is the theoretical value for a perfect control in the chain termination during polymerization. Moreover, these values indicate a greater control with both **1**,**2**/DMAP catalytic systems compared to those obtained in the presence of DMAP as organocatalyst. Besides, the polymers prepared from **1**,**2**/DMAP have a higher molar mass, suggesting that the aluminium metal complex imparts a better control of the polymerization and favors the AROP mechanism through O-alkyl bond cleavage.

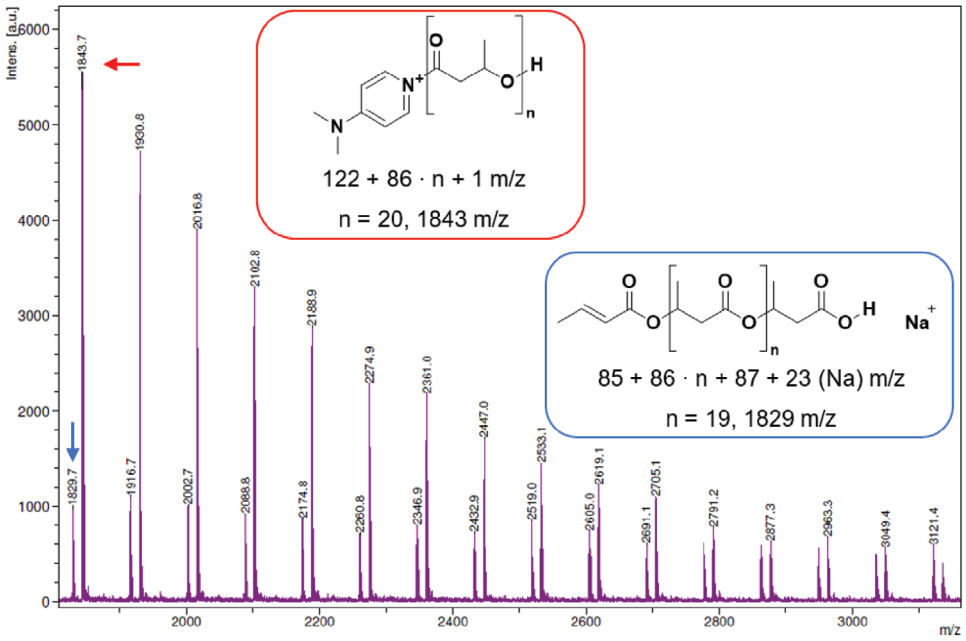

Figure 4. MALDI-TOF spectrum of a purified PHB sample prepared by ROP of BBL mediated by **1**/DMAP in bulk at 100 °C (Table 1, entry 3).

2.3. Polymerization of BPL^{OAll} Mediated by Catalyst 1

A preliminary investigation of the ROP of the *β*-functionalized propiolactone *rac*-BPL^{OAll}, mediated by catalyst **1**, was performed at NMR tube scale with a 1:10 catalyst-to-monomer ratio in C_6D_6. In the presence of an equimolar amount of BnOH, full monomer conversion was achieved at 100 °C within 3 h, thus revealing an activity similar to that observed in the ROP of BBL. Raising the temperature to 130 °C yet did not significantly improve the reaction rate. The monomer feed was then increased to 100 units (**Table 2**). The ROP performed with **1**/BnOH in toluene at 100 °C revealed very slow with a monomer conversion lower than 50%

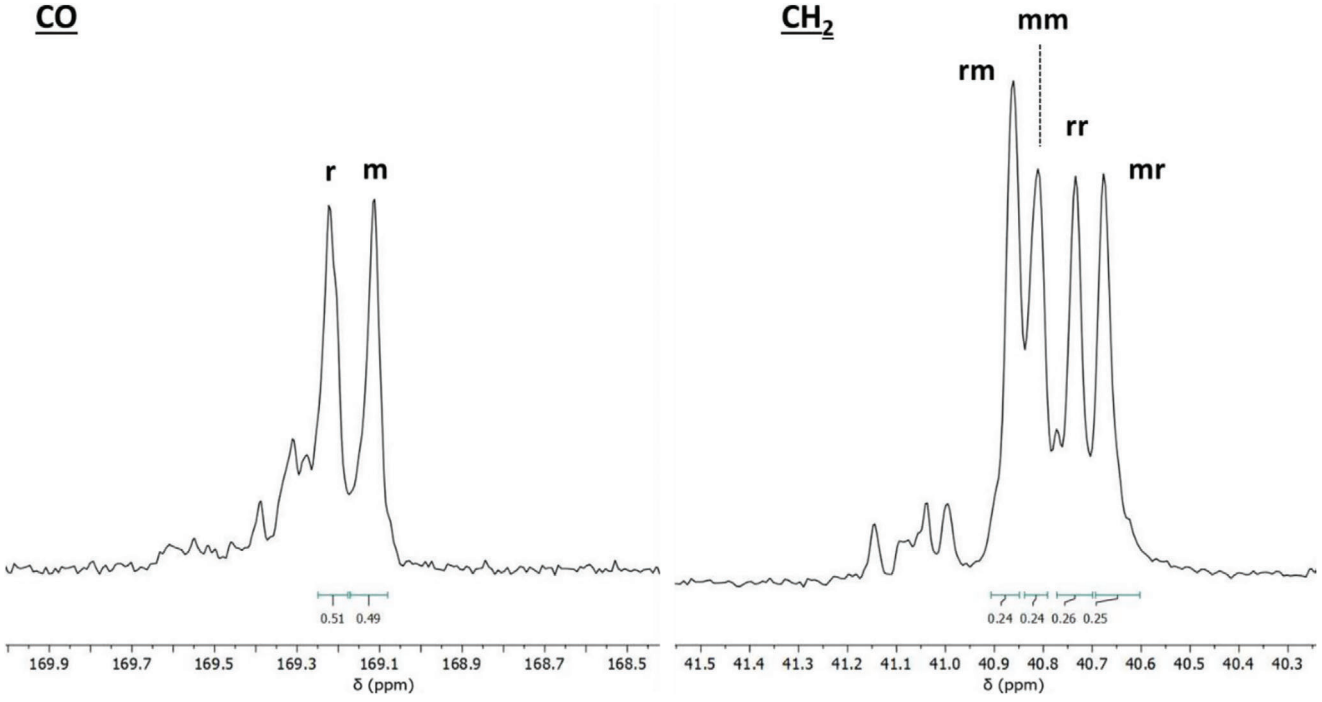

Figure 5. ^{13}C NMR regions of the methylene and carbonyl groups of the PHB samples prepared by ROP of BBL catalyzed by **1**/DMAP at 100 °C in bulk (Table 1, entry 3).

Table 2. ROP of BPL^{OAll} catalyzed by 1.

Entry	[Al]	Initiator	$[Al]_0$:$[I]_0$:$[BPL^{OAll}]_0$	Toluene [mL]	Temp. [°C]	Reaction time [h]	BPL^{OAll} Conv. [%][a)]
11	**1**	BnOH	1:1:100	0.3	100	120	49
12	**1**	BnOH	1:1:100	–	130	30	55
13	**1**	DMAP	1:1:100	–	130	2	> 99

Reaction conditions: $[Al]_0 = 20.0 \times 10^{-6}$ mol. [a)] Monomer conversion as determined by ^{1}H NMR spectroscopy.

after 2 days (Table 2, entry 11). While increasing the temperature to 130 °C facilitated the bulk polymerization, it still remained very slow. On the other hand, full conversion was achieved within 2 h when using DMAP as initiator (Table 2, entries 12–13), however only returning a short oligomer ($M_{n,SEC}$ (Da) = 750; $Đ$ = 1.53). This behavior, distinct from that of BBL, may arise from the side functional group that may be impeding the access to the catalyst metal centre.

The ^{1}H NMR spectra of the poly(*rac*-BPL^{OAll}) samples obtained with the **1**/DMAP catalytic system exhibited signals of the pyridine terminal group (**Figure 6**), as supported by the MS analysis which showed a majority of DMAP end-capped chains (Figure S17, Supporting Information). The allyloxy methyl group of the side chains seemed to hamper the formation of active crotonate species of BPL^{OAll}; hence the AROP mechanism was less favored than the reaction with **1**/DMAP and proceeded mainly through an AMM via an O-acyl ring cleavage. In fact, in the AMM mechanism the attack takes place on a carbon atom in a remote position from the side chain and could be expected to be less influenced by the allyloxy methyl group presence. The carbonyl, methine and methylene regions of the ^{13}C NMR spectrum, showed a probability to form a *racemo* diad P_r of 0.56, indicating the formation of atactic polymer samples.[79,80]

2.4. Copolymerization of BBL and BPL^{OAll} Mediated by Catalyst 1

The equimolar ROCOP of BBL with BPL^{OAll} catalyzed by **1** in the presence of BnOH, proceeded very slowly requiring 40 h to consume 80% of both monomers (**Table 3**, entry 14) (see Figure S55, Supporting Information). This ROCOP revealed significantly slower than the homopolymerization of BBL and the alike copolymerization of BBL with other substituted β-lactones.[38,53] Lowering the BPL^{OAll} loading to 10% enabled the polymerization to proceed faster, regardless of the initiator used, BnOH or DMAP (Table 3, entries 15,16). In particular, a good control in terms of molar mass values and narrow dispersity was reached using **1**/BnOH (Table 3, entry 15), while the ROCOP performed with DMAP remained sluggish (Table 3, entry 16).

Kinetic monitoring by ^{1}H NMR of the BBL/BPL^{OAll} ROCOP in a 9:1 ratio promoted by **1**/BnOH in bulk at 100 °C, revealed that,

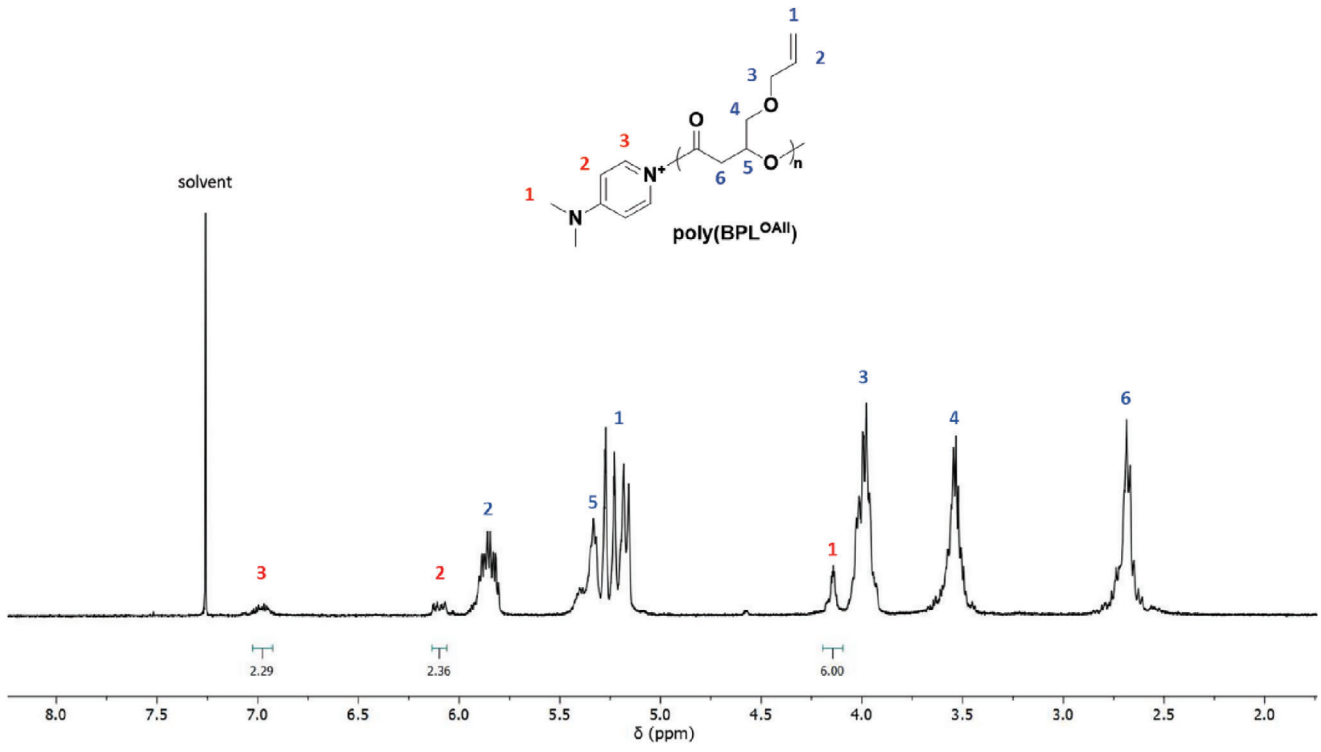

Figure 6. ^{1}H NMR spectrum (400 MHz, $CDCl_3$, 293 K) of a purified poly(BPL^{OAll}) sample end-capped with DMAP prepared by ROP of BPL^{OAll} mediated by **1**/DMAP at 130 °C in bulk (Table 2, entry 13).

Table 3. ROCOP of BPL^{OAll} and BBL catalyzed by 1 at 100 °C in bulk.

Entry	[I]	$[Al]_0$:$[I]_0$: $[BPL^{OAll}]_0$: $[BBL]_0$	Time [h]	BPL^{OAll}[a)] Conv. [%]	BBL[a] Conv. [%]	$M_{n,theo}$[b)] [kDa]	$M_{n,SEC}$[c)] [kDa]	$Đ$ [c)]
14	BnOH	1:1:50:50	40	80	80	–[d)]	–[d)]	–[d)]
15	BnOH	1:1:9:91	6	70	70	6.5	6.8	1.06
16	DMAP	1:1:9:91	2	97	99	9.2	2.8	1.11

Reaction conditions: $[Al]_0 = 20.0 \cdot 10^{-6}$ mol. [a)] Monomer conversion as determined by ^{1}H NMR analysis; [b)] Theoretical molar mass value : $M_{n,theo}$ = M (I) + [M(BBL) x 0.91 + M(BPL^{OAll}) x 0.09] x %Conv; [c)] Molar mass and dispersity as determined by SEC in THF using polystyrene standard; [d)] Not determined; not enough material was recovered from the reaction performed in an NMR tube.

at the early stage of the polymerization, both monomers were polymerized at the same rate, suggesting the formation of copolymer with $(BBL)_9(BPL^{OAll})_1$ units (Table 3, entry 16; **Figure 7**). However, after 3 h, the reaction medium became very viscous, slowing down the rate of polymerization. After 6 h, reaching ca. 70% of conversion of each monomers, the reaction medium then solidified and the polymerization stopped. The molar mass of the resulting copolymer determined by SEC then matched the expected one and showed a narrow dispersity, in agreement with a living character of the polymerization.

The ^{1}H NMR analyses of the copolymer showed 8% of BPL^{OAll} units inserted, together with the presence of a benzyloxy end-group confirming the BnOH role as initiator (**Figure 8**). The molar mass value could also be determined from the NMR analysis for this copolymer and it accounts to 7.8 KDa, in agreement with the one determined by SEC. In addition, close examination of ^{13}C NMR spectra revealed atactic polymers, as illustrated in Figure 8b (P_r = 0.4931/(0.4931 + 0.4313) = 0.53). Furthermore, the presence of only one signal for the carbonyl group of BPL^{OAll} suggested the absence of BPL^{OAll}-BPL^{OAll} adjacent units. A 2D DOSY NMR experiment displayed one diffusion coefficient for the polymer, further confirming the formation of α-allyloxy,ω-hydroxy telechelic PHB (**Figure 9**).

The MALDI-ToF mass spectrum confirmed the formation of a BBL/BPL^{OAll} copolymer enriched in BBL(91%) units. Several polymeric series are detected with the general formula $[(C_4H_6O_2)_n(C_7H_{10}O_3)_m(BnOH)Na]$ (**Figure 10**). The Gaussian curve of the polymer is centered on 5.5 kDa and reaches almost 8 kDa (see Figure S57, Supporting Information), which is in agreement with the molar mass value estimated from the NMR spectrum. The overall mass spectrum is complex, showing the partial overlap of these different series as depicted Figure 10b. An average value of 8.3% BPL^{OAll} units inserted along the PHB backbone is calculated from the experimental isotopic profiles, which matches the initial monomers loading.

3. Conclusion

Both aluminium phenoxy imine compounds $[AlXL_2]$ with X = Me (**1**) or Cl (**2**)) revealed active catalysts for the ROP of BBL in the presence of DMAP. Using BnOH as an initiator, compound **1** then showed a better control of the polymerization, while compound **2** remained inactive. The two $[AlXL_2]$/DMAP catalytic systems operated through two concomitant mechanisms returning low molar mass polymers. In both cases, the AROP mechanism initiated by an O-alkyl bond cleavage was found more prevalent, particularly for compound **2**. All the PHB revealed atactic, as evidenced by NMR studies.

Surprisingly, the ROP of the BPL^{OAll} functionalized lactone showed the opposite behavior than the one observed for the ROP of BBL using **1**/DMAP, and the **1**/BnOH catalyst system was less active, whereas it is the most efficient in the ROP of BBL. Besides, in this case, the AROP mechanism was significantly less favored, possibly arising from the presence of the functionalized group that may impede the formation of the crotonate species. This highlighted that the allyloxy functionality significantly impacted the catalytic behavior of these aluminum complexes.

Remarkably, the **1**/BnOH catalyst system afforded a well-defined functionalized PHB copolymer featuring ca. 8% of allyloxy groups along the polymer backbone. This catalytic system

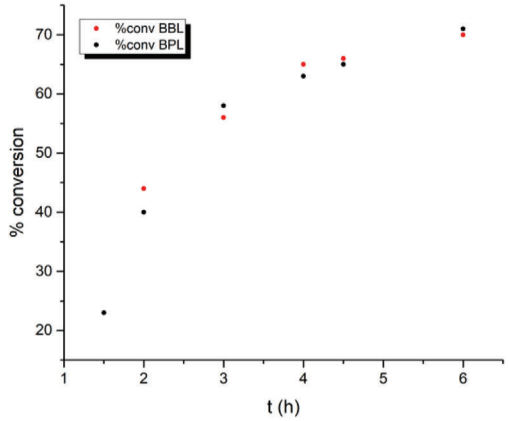

t (h)	*%conv BBL*	*%conv BPL*
1.5	23	23
2	44	40
3	56	58
4	65	63
4.5	66	65
6	68	71

Figure 7. Kinetic monitoring of the monomers conversion in the ROCOP of BBL (91 equiv.) and BPL^{OAll} (9 equiv.) mediated by **1**/BnOH in bulk at 100 °C.

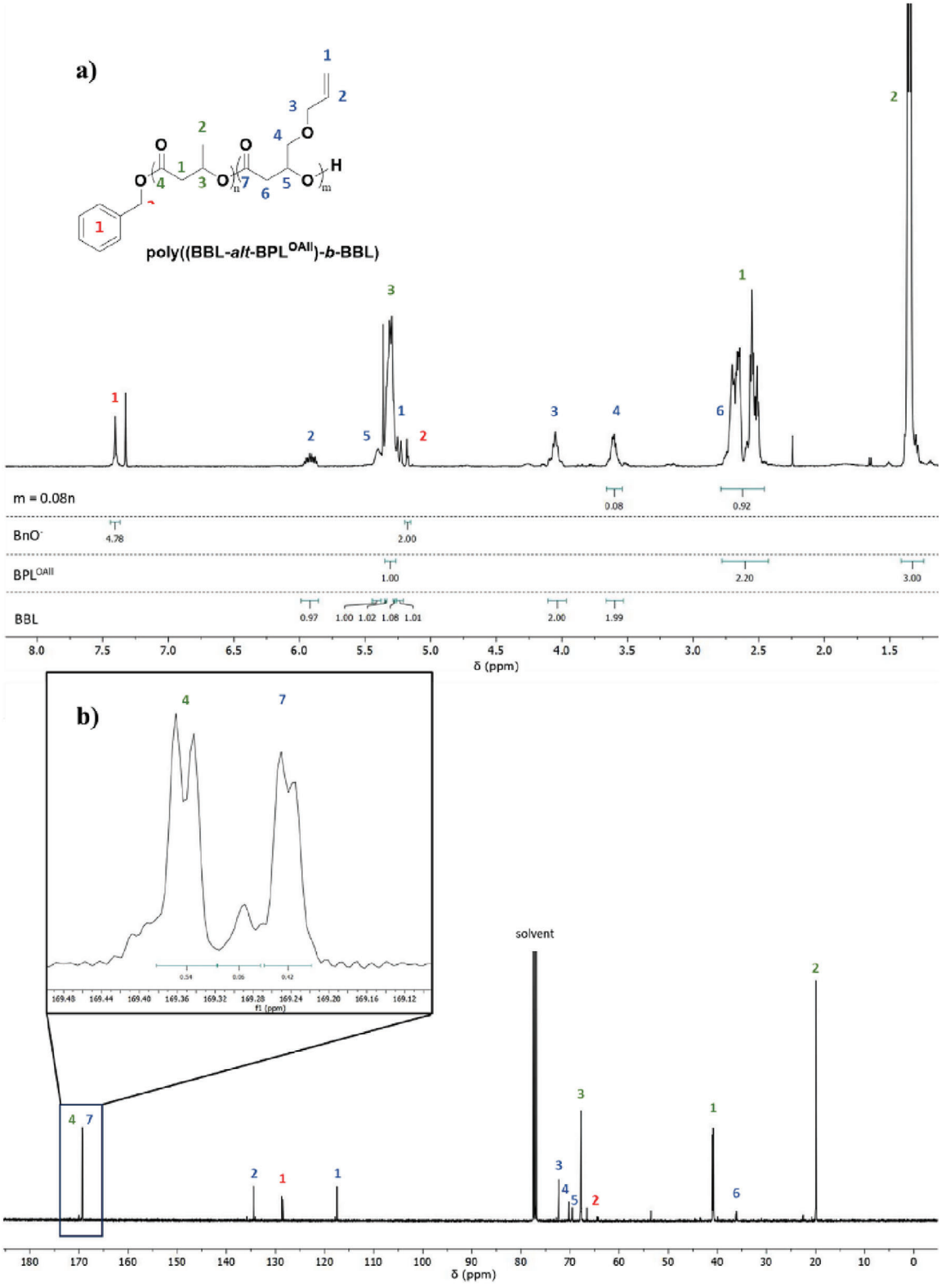

Figure 8. a) ^{1}H NMR spectrum (400 MHz, $CDCl_3$, 293 K) and b) ^{13}C NMR spectrum with the expanded region of the carbonyl groups of the purified poly((BBL-*alt*-BPL^{OAll})-*b*-BBL) isolated from the ROCOP of BBL (91 equiv.) and BPL^{OAll} (9 equiv.) in bulk at 100 °C catalyzed by **1**/BnOH (Table 3, entry 15).

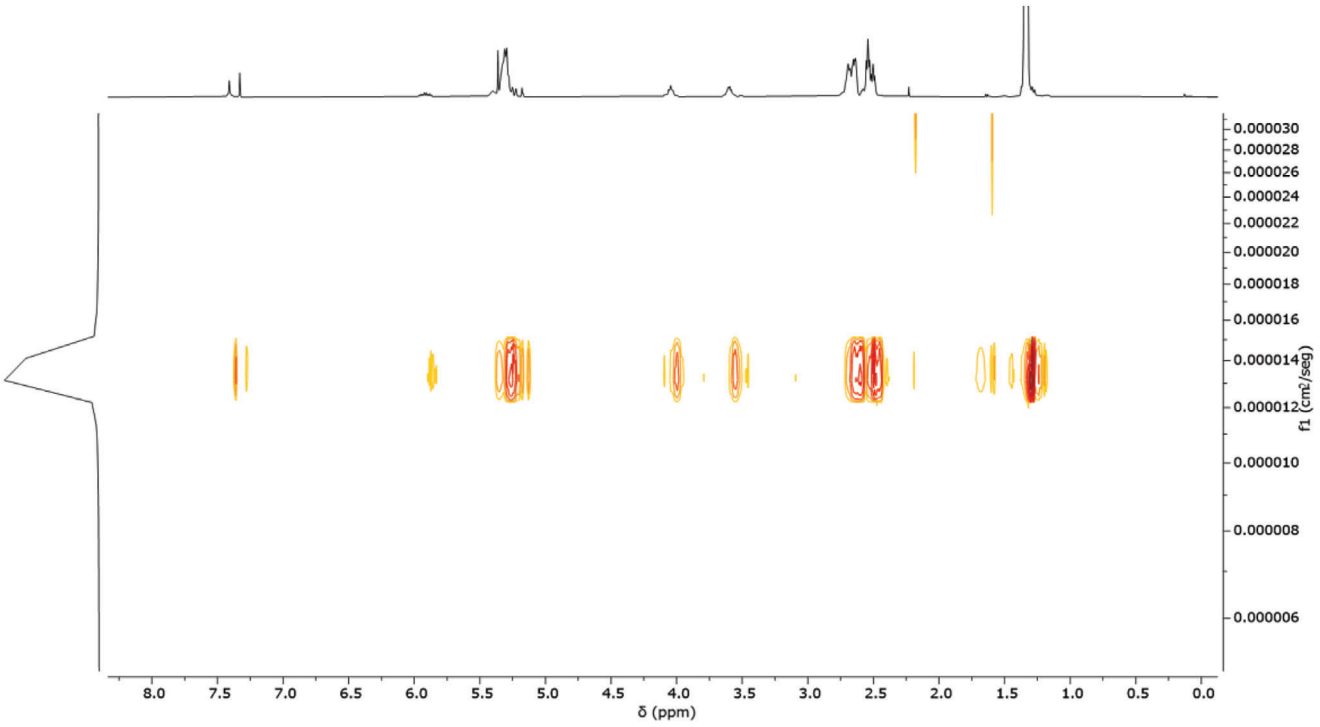

Figure 9. DOSY NMR spectrum (400 MHz, $CDCl_3$, 293 K) of the purified poly((BBL-*alt*-BPL^{OAll})-*b*-BBL) of the ROCOP of BBL (91 equiv.) and BPL^{OAll} (9 equiv.) performed in bulk at 100 °C catalyzed by **1**/BnOH (Table 3, entry 15).

once again showed higher activity, achieving also a greater control over the process. The allyloxy substituents did not undergo any side reactions during the ROCOP process and pave the way to post-polymerization modifications toward more sophisticated polymers.

4. Experimental Section

Methods and Materials: All manipulations were carried out under inert atmosphere of argon using standard Schlenk and glovebox techniques. All solvents were rigorously dried prior to use following standard methods. NMR spectra were recorded from a Bruker 400 Ultrashield (^{1}H 400 MHz, ^{13}C 101 MHz) at room temperature. Assignment of signals was carried out from 1D (^{1}H, $^{13}C\{^1H\}$) and 2D (^{1}H—^{13}C HSQC, HMBC) NMR experiments. The molar masses (M_n and M_w) and dispersities (M_w/M_n) of polymer samples were determined by size exclusion chromatography (SEC) at 25 °C using THF as solvent with a flow rate of the eluent of 1 mL·min^{-1}, and using polystyrene standard as calibrants. MALDI-TOF MS analysis was performed on an ULTRAFLEX III TOF/TOF from Bruker. The ionization system used was a matrix of *trans*-2-[3-(4-*tert*-butylphenyl)−2-methyl-2-propenylidene]malononitrile (DCTB) doped with sodium iodide to promote the formation of [M+Na$^+$] molecular ions. All data enabled the characterization the polymers (micro)structure.

BBL was purchased from Aldrich and then purified by vacuum distillation with CaH_2 and stored under argon. DMAP was purchased from Aldrich and then purified by recrystallization in dry toluene. BPL^{OAll} was synthesized as described in the literature.[81] The other reagents were commercially obtained and used without further purification. $[AlMe_2\{2,6\text{-}(CHPh_2)_2\text{-}4\text{-}^tBu\text{-}C_6H_2O\}]_n$, 2,6-^{i}Pr$_2C_6H_3$N=CH-C$_6H_4$OH (LH) and [AlMeL$_2$] were prepared according to reported methods.[38]

Synthesis of [AlCl{(O-2-(2,6-^{i}Pr$_2$C$_6$H$_3$)N=CHC$_6$H$_4$)}$_2$] (2): A solution containing LH (0.79 g, 2.80 mmol) in toluene (30 mL) was prepared. To this solution, dimethylaluminium chloride ($AlClMe_2$) (1.56 mL, 1.40 mmol) was added at −78 °C. The resulting mixture was stirred for 40 min at this temperature before allowing it to warm up to room temperature. Subsequently, the solution was concentrated until a yellow powder precipitated Crystals of **2** were isolated following a brief reflux and storage at −20 °C. Yellow crystals suitable for single-crystal X-ray diffraction were obtained within 48 h (0.80 g, 87% yield). ^{1}H NMR (400 MHz, 293 K, C_6D_6): δ (ppm) 0.97 (d, 6H, ^3J = 7 Hz, HC(C*H*$_3$)$_2$,), 1.16 (d, 6H, ^3J = 7 Hz, HC(C*H*$_3$)$_2$), 1.22 (d, 6H, ^3J = 7 Hz, HC(C*H*$_3$)$_2$), 1.44 (d, 6H, ^3J = 7 Hz, HC(C*H*$_3$)$_2$), 3.16 (m, 2H, ^3J = 7 Hz, *H*C(CH$_3$)$_2$), 3.87 (m, 2H, ^3J = 7 Hz, *H*C(CH$_3$)$_2$), 6.12 (m, 2H, ^3J = 8 Hz, Ar*H*), 6.42 (m, 2H, ^3J = 8 Hz, Ar*H*), 6.76 (m, 2H, ^3J = 8 Hz, Ar*H*), 6.95 (m, 2H, ^3J = 8 Hz, Ar*H*), 7.14 (m, 2H, Ar*H*), 7.29 (m, 4H, ^3J = 4 Hz, Ar*H*), 7.98 (s, 2H, *H*C = N). ^{13}C NMR (100.6 MHz, 293 K, C_6D_6): δ (ppm) 22.71 (HC(*C*H$_3$)$_2$), 24.74 (HC(*C*H$_3$)$_2$), 25.20 (HC(*C*H$_3$)$_2$), 25.26 (HC(*C*H$_3$)$_2$), 28.28 (*H*C(CH$_3$)$_2$), 29.87 (*H*C(CH$_3$)$_2$), 118.21 (Ar—*C*), 121.61 (Ar—*C*), 123.00 (Ar—*C*), 124.50 (Ar—*C*), 133.50 (Ar—*C*), 136.46 (Ar—*C*), 119.77, 125.70, 126.83, 128.57, 129.33, 141.75, 142.53, 148.54 ($C_{quaternary}$) 164.43 (*C*—O), 172.23 (HC = N). Anal. Calc. (%) for $AlC_{38}H_{44}N_2O_2Cl$ (623.23 g mol^{-1}): C, 73.23; H, 7.06. Exp.: C, 73.65; H, 6.97.

Typical Polymerization Procedure: Inside the glovebox, the required amount of catalyst was weighted and placed in a Schlenk flask equipped with a magnetic stirr bar. Then, the measured volume of monomer was charged inside the flask, that was next submerged in an oil bath at the desired temperature, outside the glovebox. After the desired reaction time, the flask was removed from the bath, opened to the air and poured over three volumes of "wet" hexane to precipitate the polymer. Before quenching, aliquots were taken to determine the monomer conversion and polymer formation by NMR spectroscopy. The recovered polymers were characterized by FTIR and NMR spectroscopies, mass spectrometry, and SEC analysis.

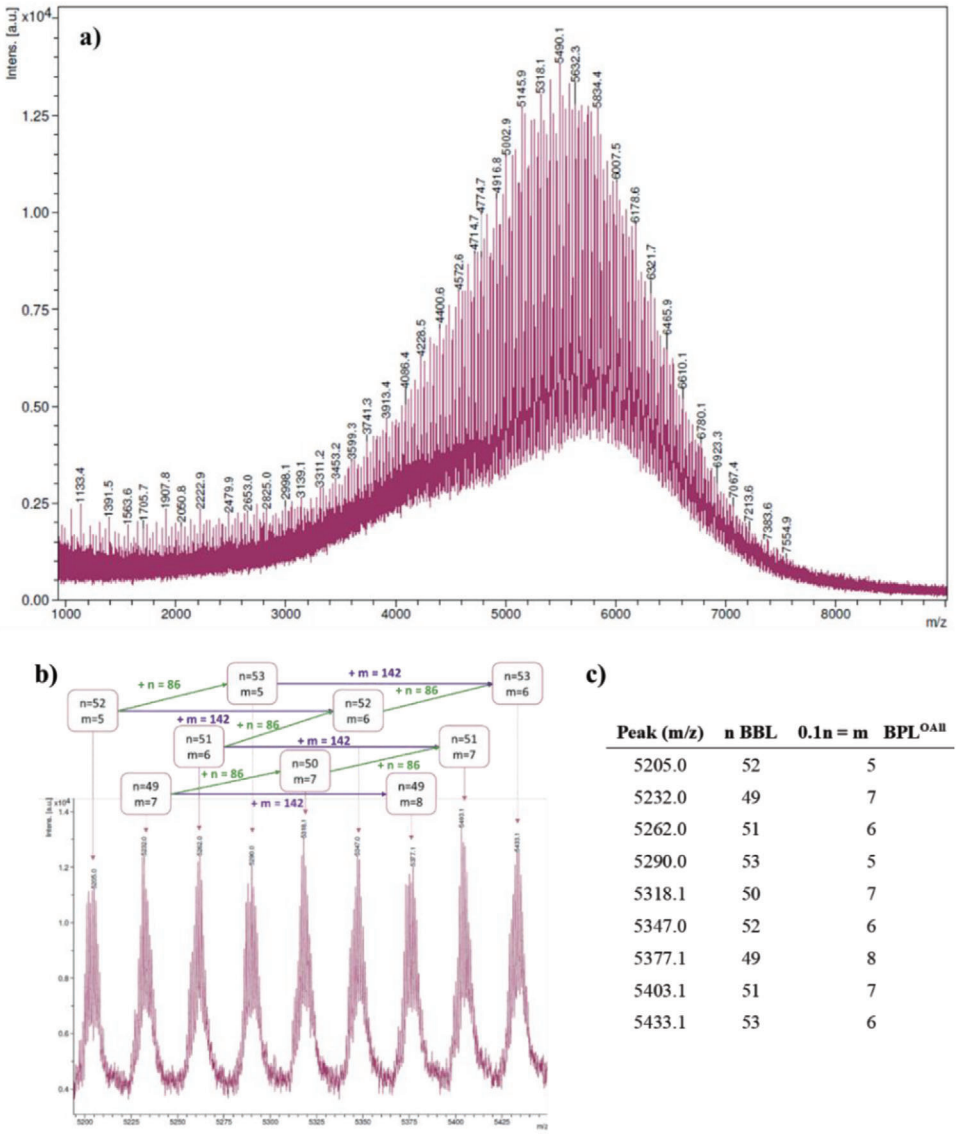

Peak (m/z)	n BBL	0.1n = m	BPL^{OAll}
5205.0	52		5
5232.0	49		7
5262.0	51		6
5290.0	53		5
5318.1	50		7
5347.0	52		6
5377.1	49		8
5403.1	51		7
5433.1	53		6

Figure 10. a) MALDI-ToF mass spectrum of poly((BBL-*alt*-BPL^{OAll})-*b*-BBL) and b) expansion of the spectrum along with c) experimental and calculated polymer series containing different ratios of BPL^{OAll}.

X-Ray Studies of Compound 2: Data collection was performed at 200(2) K, with the crystals covered with perfluorinated ether oil. A single crystal of **2** was mounted on a Bruker–Nonius Kappa CCD single crystal diffractometer equipped with a graphite-monochromated Mo-Kα radiation (λ = 0.71073 Å). Multiscan[82] absorption correction procedures were applied to the data. The structure was solved using the WINGX package,[83] by direct methods (SHELXS-13) and refined using full-matrix least-squares against F^2 (SHELXL-16).[84] All non-hydrogen atoms were anisotropically refined. Hydrogen atoms were geometrically placed and left riding on their parent atoms, except for the ones bonded to C32, C21 and C54, and the ones bonded to the aromatic ring of the toluene. In the asymmetric unit cell there are 1.5 molecules and one toluene that shows some disorder. The half molecule is also disordered and the oxygen atom of the ligand has been refined in two positions. Full-matrix least-squares refinements were carried out by minimizing $\sum w(Fo^2 - Fc^2)$[2] with the SHELXL-16 weighting scheme and stopped at shift/err < 0.001. The final residual electron density maps showed no remarkable features. Crystallographic data for the structure reported in this paper have been deposited with the Cambridge Crystallographic Data Centre as supplementary publication number CCDC: 2 331 618

Supporting Information

Supporting Information is available from the Wiley Online Library or from the author.

Acknowledgements

This research was supported by Ministerio de Ciencia e Innovación (Spain) (PID2021-122708OB-C31 and AEI/10.13039/501100011033), Comunidad de Madrid (EPU-INV/2020/001), and the University of Alcalá (UAH-AE-2017-2 and PIUAH23/CC-046). V.S. would like to thank the Ministerio de Ciencia e Innovación (Spain) and the European Community (grant number: RYC2021-033921-I) for the financial support. M.P. would like to thank University of Alcalá for a fellowship.

Conflict of Interest

The authors declare no conflict of interest.

Data Availability Statement

The data that support the findings of this study are available from the corresponding author upon reasonable request.

Keywords

aluminum catalyst, BBL, DMAP, functionalized PHB, ring-opening polymerization, ROP

Received: February 13, 2024
Revised: April 22, 2024
Published online: May 11, 2024

[1] M. S. Kim, H. Chang, L. Zheng, Q. Yan, B. F. Pfleger, J. Klier, K. Nelson, E. L. W. Majumder, G. W. Huber, *Chem. Rev.* **2023**, *123*, 9915.
[2] A. K. Mohanty, F. Wu, R. Mincheva, M. Hakkarainen, J. M. Raquez, D. Mielewski, R. Narayan, A. N. Netravali, M. Misra, *Nat. Rev. Methods Primers* **2022**, *2*, 46.
[3] F. Guzmán-Lagunes, P. Wongsirichot, J. Winterburn, C. Guerrero Sanchez, C. Montiel, *Ind. Eng. Chem. Res.* **2023**, *62*, 18133.
[4] K. Sudesh, H. Abe, Y. Doi, *Prog. Polym. Sci.* **2000**, *25*, 1503.
[5] R. W. Lenz, R. H. Marchessault, *Biomacromolecules* **2005**, *6*, 1.
[6] J. Lu, R. C. Tappel, C. T. Nomura, *Polym. Rev.* **2009**, *49*, 226.
[7] S. Taguchi, T. Iwata, H. Abe, Y. Doi, in *Polymer Science: A Comprehensive Reference*, Elsevier, Amsterdam, **2012**.
[8] M. L. Iglesias-Montes, M. Soccio, F. Luzi, D. Puglia, M. Gazzano, N. Lotti, L. B. Manfredi, V. P. Cyras, *Polymers* **2021**, *13*, 3171.
[9] M. Suzuki, Y. Tachibana, K.-I. Kasuya, *Polym. J.* **2021**, *53*, 47.
[10] A. Dhaini, V. Hardouin-Duparc, A. Alaaeddine, J. F. Carpentier, S. M. Guillaume, *Prog. Polym. Sci.* **2024**, *149*, 101781.
[11] G. Q. Chen, *Chem. Soc. Rev.* **2009**, *38*, 2434.
[12] M. Kumar, R. Rathour, R. Singh, Y. Sun, A. Pandey, E. Gnansounou, K. Y. Andrew Lin, D. C. W. Tsang, I. S. Thakur, *J. Clean Prod.* **2020**, *263*, 121500.
[13] V. Sessini, S. Ghosh, M. E. G. Mosquera, in *Biopolymers: 3171 Synthesis, Properties, and Emerging Applications*, Elsevier, Amsterdam, **2023**.
[14] X. Tang, E. Y. Chen, *Nat. Commun.* **2018**, *9*, 2345.
[15] A. H. Westlie, E. C. Quinn, C. R. Parker, E. Y. X. Chen, *Prog. Polym. Sci.* **2022**, *134*, 101608.
[16] D. Sanchez-Roa, V. Sessini, M. E. G. Mosquera, J. Cámpora, *ACS Catal.* **2024**, *14*, 2487.
[17] R. Reichardt, B. Rieger, in *Synthetic Biodegradable Polymers*, Springer, Berlin, Heidelberg, **2012**.
[18] D. M. Lyubov, A. O. Tolpygin, A. A. Trifonov, *Coord. Chem. Rev.* **2019**, *392*, 83.
[19] H. Li, R. M. Shakaroun, S. M. Guillaume, J. F. Carpentier, *Chem. - Eur. J.* **2020**, *26*, 128.
[20] L. Zhou, Z. Zhang, C. Shi, M. Scoti, D. K. Barange, R. R. Gowda, E. Y. X. Chen, *Science* **2023**, *380*, 64.
[21] N. Ajellal, M. Bouyahyi, A. Amgoune, C. M. Thomas, A. Bondon, I. Pillin, Y. Grohens, J. F. Carpentier, *Macromolecules* **2009**, *42*, 987.
[22] J. F. Carpentier, *Macromol. Rapid Commun.* **2010**, *31*, 1696.
[23] D. Pappalardo, M. Bruno, M. Lamberti, C. Pellecchia, *Macromol. Chem. Phys.* **2013**, *214*, 1965.
[24] J. Bruckmoser, S. Pongratz, L. Stieglitz, B. Rieger, *J. Am. Chem. Soc.* **2023**, *145*, 11494.
[25] J. Bruckmoser, S. Pongratz, B. Rieger, *Organometallics* **2023**, *42*, 876.
[26] E. Grunova, E. Kirillov, T. Roisnel, J. F. Carpentier, *Dalton Trans.* **2010**, *39*, 6739.
[27] B. J. Jeffery, E. L. Whitelaw, D. Garcia-Vivo, J. A. Stewart, M. F. Mahon, M. G. Davidson, M. D. Jones, *Chem. Commun.* **2011**, *47*, 12328.
[28] E. Luciano, A. Buonerba, A. Grassi, S. Milione, C. Capacchione, *J. Polym. Sci., Part A: Polym. Chem.* **2016**, *54*, 3132.
[29] M. Zintl, F. Molnar, T. Urban, V. Bernhart, P. Preishuber-Pflügl, B. Rieger, *Angew. Chem., Int. Ed.* **2008**, *47*, 3458.
[30] R. Reichardt, S. Vagin, R. Reithmeier, A. K. Ott, B. Rieger, *Macromolecules* **2010**, *43*, 9311.
[31] J. E. Kemnitzer, S. P. McCarthy, R. A. Gross, *Macromolecules* **1993**, *26*, 6143.
[32] J. E. Kemnitzer, S. P. McCarthy, R. A. Gross, *Macromolecules* **1993**, *26*, 1221.
[33] H. R. Kricheldorf, S. R. Lee, N. Scharnagl, *Macromolecules* **1994**, *27*, 3139.
[34] H. R. Kricheldorf, S. Eggerstedt, *Macromolecules* **1997**, *30*, 5693.
[35] Y. Hori, T. Hagiwara, *Int. J. Biol. Macromol.* **1999**, *25*, 237.
[36] S. Hiki, M. Miyamoto, Y. Kimura, *Polymer* **2000**, *41*, 7369.
[37] L. R. Rieth, D. R. Moore, E. B. Lobkovsky, G. W. Coates, *J. Am. Chem. Soc.* **2002**, *124*, 15239.
[38] F. M. García-Valle, V. Tabernero, T. Cuenca, M. E. G. Mosquera, J. Cano, S. Milione, *Organometallics* **2018**, *37*, 837.
[39] N. Nomura, T. Aoyama, R. Ishii, T. Kondo, *Macromolecules* **2005**, *38*, 5363.
[40] M. P. F. Pepels, M. Bouyahyi, A. Heise, R. Duchateau, *Macromolecules* **2013**, *46*, 4324.
[41] C. Agatemor, A. E. Arnold, E. D. Cross, A. Decken, M. P. Shaver, *J. Organomet. Chem.* **2013**, *745–746*, 335.
[42] E. D. Cross, L. E. N. Allan, A. Decken, M. P. Shaver, *J. Polym. Sci., Part A: Polym. Chem.* **2013**, *51*, 1137.
[43] X. X. Zheng, Z. X. Wang, *RSC Adv.* **2017**, *7*, 27177.
[44] S. Impemba, G. Manca, I. Tozio, S. Milione, *Polymers* **2023**, *15*, 4366.
[45] J. Bruckmoser, D. Henschel, S. Vagin, B. Rieger, *Catal. Sci. Technol.* **2022**, *12*, 3295.
[46] Z. Zhou, A. M. LaPointe, G. W. Coates, *J. Am. Chem. Soc.* **2023**, *145*, 25983.
[47] G. Barouti, S. M. Guillaume, *Polym. Chem.* **2016**, *7*, 4603.
[48] G. Barouti, K. Jarnouen, S. Cammas-Marion, P. Loyer, S. M. Guillaume, *Polym. Chem.* **2015**, *6*, 5414.
[49] G. Barouti, S. S. Liow, Q. Dou, H. Ye, C. Orione, S. M. Guillaume, X. J. Loh, *Chem. - Eur. J.* **2016**, *22*, 10501.
[50] S. M. Guillaume, E. Kirillov, Y. Sarazin, J. F. Carpentier, *Chem. - Eur. J.* **2015**, *21*, 7988.
[51] C. Gallegos, V. Tabernero, F. M. Garcıá-Valle, M. E. G. Mosquera, T. Cuenca, J. Cano, *Organometallics* **2013**, *32*, 6624.
[52] F. M. García-Valle, V. Tabernero, T. Cuenca, J. Cano, M. E. G. Mosquera, *Dalton Trans.* **2018**, *47*, 6499.
[53] F. M. García-Valle, T. Cuenca, M. E. G. Mosquera, S. Milione, J. Cano, *Eur. Polym. J.* **2020**, *125*, 109527.
[54] F. M. García-Valle, R. Estivill, C. Gallegos, T. Cuenca, M. E. G. Mosquera, V. Tabernero, J. Cano, *Organometallics* **2015**, *34*, 477.
[55] E. E. Marlier, J. A. Macaranas, D. J. Marell, C. R. Dunbar, M. A. Johnson, Y. DePorre, M. O. Miranda, B. D. Neisen, C. J. Cramer, M. A. Hillmyer, W. B. Tolman, *ACS Catal.* **2016**, *6*, 1215.
[56] D. E. Stasiw, M. Mandal, B. D. Neisen, L. A. Mitchell, C. J. Cramer, W. B. Tolman, *Inorg. Chem.* **2017**, *56*, 725.
[57] B. Wang, Y. Wei, Z. J. Li, L. Pan, Y. S. Li, *ChemCatChem* **2018**, *10*, 5287.
[58] J. H. Wang, C. Y. Tsai, J. K. Su, B. H. Huang, C. C. Lin, B. T. Ko, *Dalton Trans.* **2015**, *44*, 12401.
[59] T. Feng, D. Bu, H. Lei, *Polyhedron* **2018**, *148*, 109.
[60] N. Iwasa, S. Katao, J. Liu, M. Fujiki, Y. Furukawa, K. Nomura, *Organometallics* **2009**, *28*, 2179.

[61] J. Ternel, P. Roussel, F. Agbossou-Niedercorn, R. M. Gauvin, *Catal. Sci. Technol.* **2013**, *3*, 580.
[62] M. S. Hill, A. R. Hutchison, T. S. Keizer, S. Parkin, M. A. VanAelstyn, D. A. Atwood, *J. Organomet. Chem.* **2001**, *628*, 71.
[63] C. R. Groom, I. J. Bruno, M. P. Lightfoot, S. C. Ward, *Acta Cryst. B* **2016**, *72*, 171.
[64] A. Amgoune, C. M. Thomas, S. Ilinca, T. Roisnel, J. F. Carpentier, *Angew. Chem., Int. Ed.* **2006**, *45*, 2782.
[65] K. Nie, L. Fang, Y. Yao, Y. Zhang, Q. Shen, Y. Wang, *Inorg. Chem.* **2012**, *51*, 11133.
[66] E. Luciano, A. Buonerba, A. Grassi, S. Milione, C. Capacchione, *J. Polym. Sci., Part A: Polym. Chem.* **2016**, *54*, 3132.
[67] H. Wang, J. Guo, Y. Yang, H. Ma, *Dalton Trans.* **2016**, *45*, 10942.
[68] Z. Jedliński, M. Kowalczuk, P. Kurcok, *Die Makromolekulare Chemie* **1986**, *3*, 277.
[69] Z. Jedliński, P. Kurcok, M. Kowalczuk, J. Kasperczyk, *Makromol. Chem.* **1986**, *187*, 1651.
[70] A. Khalil, S. Cammas-Marion, O. Coulembier, *Polym. Chem.* **2019**, *57*, 657.
[71] G. Adamus, A. Domiński, M. Kowalczuk, P. Kurcok, I. Radecka, *Polymers* **2021**, *13*, 4365.
[72] Y. Yamashita, K. Ito, F. Nakakita, *Die Makromolekulare Chemie* **1969**, *127*, 292.
[73] M. Shaik, J. Peterson, G. Du, *Macromolecules* **2019**, *52*, 157.
[74] H. R. Kricheldorf, N. Scharnagl, *J. Macromol. Sci. Chem., A* **1989**, *26*, 951.
[75] F. Isnard, F. Santulli, M. Cozzolino, M. Lamberti, C. Pellecchia, M. Mazzeo, *Catal. Sci. Technol.* **2019**, *9*, 3090.
[76] J. E. Kemnitzer, S. P. McCarthy, R. A. Gross, *Macromolecules* **1993**, *26*, 6143.
[77] E. Caytan, R. Ligny, J. F. Carpentier, S. M. Guillaume, *Polymers* **2018**, *10*, 533.
[78] J. E. Kemnitzer, S. P. McCarthy, R. A. Gross, *Macromolecules* **1992**, *25*, 5927.
[79] R. Ligny, M. M. Hänninen, S. M. Guillaume, J. F. Carpentier, *Angew. Chem., Int. Ed.* **2017**, *56*, 10388.
[80] R. M. Shakaroun, P. Jéhan, A. Alaaeddine, J. F. Carpentier, S. M. Guillaume, *Polym. Chem.* **2020**, *11*, 2640.
[81] J. A. R. Schmidt, E. B. Lobkovsky, G. W. Coates, *J. Am. Chem. Soc.* **2005**, *127*, 11426.
[82] R. Blessing, *Acta Cryst. A* **1995**, *51*, 33.
[83] L. Farrugia, *J. Appl. Crystallogr.* **1999**, *32*, 837.
[84] G. A. Sheldrick, *Acta Cryst. A* **2008**, *64*, 112.